Hindawi
Advances in Materials Science and Engineering
Volume 2020, Article ID 3826128, 12 pages
https://doi.org/10.1155/2020/3826128

Research Article

Estimating Deterioration Rate of Some Carbonate Rocks Used as Building Materials under Repeated Frost Damage Process, China

Marzouk Mohamed Aly Abdelhamid,[1,2] **Dong Li**,[1] **Gaofeng Ren**,[1,3] **and Congrui Zhang**[1,3]

[1]*Wuhan University of Technology, School of Resources and Environmental Engineering, Luoshi Road 122, Wuhan, Hubei 430070, China*
[2]*Al-Azhar University, Faculty of Engineering, Mining and Petroleum Engineering Department, Cairo, Egypt*
[3]*Key Laboratory of Mineral Resources Processing and Environment of Hubei Province, Luoshi Road 122, Wuhan, Hubei 430070, China*

Correspondence should be addressed to Gaofeng Ren; rgfwhut@163.com and Congrui Zhang; zcrwhut@163.com

Received 26 October 2019; Accepted 24 December 2019; Published 20 January 2020

Academic Editor: Ivan Giorgio

The degradation of natural rocks due to severe environmental conditions can influence their durability over an extended period of time. This research aims to investigate the long-term durability or disintegration rate of rocks used as construction materials under severe climatic conditions using frost damage action, and the deterioration rate was assessed using mathematical decay function approach. The mathematical model assumes an initial order operation and gives purposeful properties for the deterioration rate of rocks due to frost action. For this reason, six different limestone types used as building materials were quarried from limestone mine in China and subjected to a series of laboratory tests to determine the mineralogical, petrographical, physical, and mechanical characteristics. Then, 50 cycles of frost damage process was performed, and after each 10 cycles, the unconfined compressive strength, point load strength, and Schmidt rebound were determined. The disintegration rate or integrity loss characteristics of each rock type were assessed using the mathematical decay function approach parameters. This approach proved that the disintegration rate varies for the rocks of the same type especially which were extracted from the same areas, the rock durability under frost damage conditions can be estimated with good accuracy, the parameters of this model saved a lot of time and provided important practical features to assess a rapid durability, and hence, there is no need to carry out the frost damage test which is slow and consumes time.

1. Introduction

Natural rocks have commonly been used as building stones and construction materials in many engineering projects [1] especially in historical monuments and modern buildings from past until present times [2]. Natural stones and marbles have widely been used as building or decorative materials in outdoor applications such as cladding the outsides of buildings walls and for structural applications (paves, columns, and floors) [3]. The rock durability is defined as its resistance to environmental conditions over an extended period of time. The artificial weathering processes play an important role in influencing the characteristics of rock materials [4]. Frost-induced action has been viewed as an important weathering test and one of the first ones that historically was used to determine the efficiency of building and construction materials. In addition, the rock breakage or deterioration due to artificial weathering processes is very significant in many engineering applications, such as railways, roads, and in cold areas [5, 6].

Frost action is one of the most powerful natural degradation processes for natural rocks [7] in which building stones experience frost-weathering cycles when they are used in the moist environmental conditions in which the temperature repeatedly changes up and below freezing point of water [8]. When water turns into ice, it expands in volume by about 9%; hence, it will generate increased pressure inside the pores. When the stress exceeds than the rock tensile

strength, new microcracks or fissures are formed and the present ones are widened and deepened; therefore, these fluctuations can influence the rock mechanical characteristics, and thus, the durability of the stone becomes limited [9]. Frost-weathering cycles can cause rapid variations in physical and mechanical parameters; as a result, the rock durability is influenced [10, 11]. Therefore, it is required to identify the disintegration rate of natural rocks under frost-weathering conditions.

Many studies have investigated the durability, in addition the physical and mechanical parameters of different rocks against frost-weathering action [12–20]. Jamshidi et al. [12], Di Benedetto et al. [13], and Vázquez et al. [14] used some criteria according to physical-mechanical properties of building stones as durability estimators. Bayram [15] proposed a statistical model to assess the rate of decrease values in unconfined compressive strength. Karaca et al. [16] experimentally investigated the Böhme abrasion and wide-wheel abrasion parameters before and after frost-weathering tests. They proposed the statistical models for the results of abrasion test before and after frost cycles. Tan et al. [17] studied the degradation in the mechanical parameters of granite as a function of freezing-thawing weathering processes by triaxial and uniaxial compression tests. Takarli et al. [10] studied the influence of frost-weathering cycles on microstructure in saturated granitic rocks by testing compression pulse velocity and permeability. They postulated that compressional pulse velocity measurement could provide an assessment of total degradation and the permeability test could give an evaluation of specific decay depending on porous network changes in rocks. Yavuz et al. [18] postulated a model equation for predicting the index parameters of carbonate rocks against frost cycles. This equation indicates reduction in the index parameter of a deteriorated rock according to its initial parameter and porosity of rock with the coefficients for a special index parameter. Sousa et al. [19] derived an empirical formula to relate rock strength to porosity for granitic rock samples. Mutlutürk et al. [20] proposed a decay function model characterizing the long-term durability using only the physical property (shore hardness) of natural rocks due to frost action, and it provided different meaningful factors for rock durability. In spite of most of the previous researches, different methods of the influences of frost-weathering process on the rocks have been studied for many times; however, the numerical modeling methods are not enough to estimate the deterioration rate of rocks used as building stones and construction materials under frost-weathering conditions [15, 18, 20].

The main objectives of this study are to (1) investigate the long-term durability of different limestone types used as building stones and construction materials subject to severe environmental conditions by using frost damage process; (2) estimate the integrity loss or deterioration rate of rocks depending on the mathematical decay function approach using unconfined compressive strength, point load strength, and Schmidt hammer rebound; and (3) determine whether the different rocks of the same type can provide sufficient information according to their durability under frost damage condition action or not.

2. Materials and Methods

2.1. Materials Used Description. In this study, six different limestone types were taken out from various layers of limestone rock mine near Jingzhou, Songzi, Hubei, China (Figure 1). All these studied rocks are commonly commercialized as building stones and construction materials. The rock cores were taken out from large blocks with dimensions of $40 \times 40 \times 30$ cm and prepared in a cylindrical shape with a diameter of 50 mm (Figure 2) with a total of 110 samples being obtained. The selection of these specimens was free from any defects such as cracks or fractures, bedding planes, and deterioration to avoid the impact of anisotropy on the measurement. The mineral composition and microstructure features of the studied rock samples were determined using a polarized microscope. Two series of rock specimens were prepared in this research; one set of these specimens was used to determine the initial physicomechanical characteristics including dry and saturated bulk density; water absorption; effective porosity; unconfined compressive index strength; point load strength; and Schmidt hammer rebound before frost damage cycles. The second set of the studied rock specimens was subjected to 50 cycles of frost damage to determine the mechanical strength parameters including unconfined compressive strength, point load strength, and Schmidt hammer rebound. Finally, their long-term durability or deterioration rate due to frost damage conditions was estimated according to the mathematical decay function model.

2.2. Petrographic Analysis. Determining the petrographic features provides enough information on the mineral composition and provenance of origin of natural rock; in addition, it is considered as a significant tool for estimating the durability of rocks and resistance due to deterioration or weathering agents. In this study, the polarized microscope was used to identify the microstructure characteristics of the specimens (Figure 3). As shown in Figure 3, the microstructure features of limestone type 1 is fine grained, composed mainly of calcite as major mineral constituent associated with some rare amounts of opaque minerals. Calcite presents as a fine euhedral crystal; limestone type 2 is fine to medium grain, composed mainly of calcite as essential component and represented the cement of the rock with rare amounts of opaque minerals. Calcite presents as fine to medium euhedral interlocked crystals; limestone type 3 is fine to medium grain, consisting mainly of calcite as major mineral constituent associated with some accessory minerals such as hydromagnesite and talc less than 6%. Talc occurs as medium anhedral grain outlines in the matrix of calcite; limestone type 4 is fine grained, composed mainly of calcite as main mineral constituent associated with some rare amounts of quartz mineral and talc minerals less than 5%. Quartz occurs as fine to medium grains. Talc occurs as fine anhedral grained texture. Very fine fossils were observed in this rock; limestone type 5 is fine grained, consisting mainly of calcite as main mineral constituent associated with some rare amounts of opaque minerals. Some parts of the

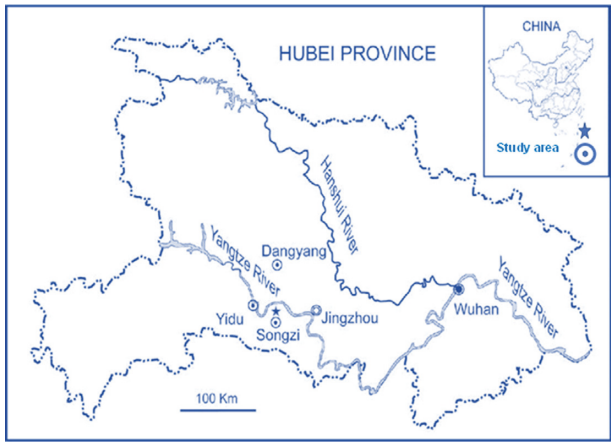

Figure 1: Location map of the studied limestone mine sample site in China.

Figure 2: Some of the prepared core rock samples under study.

rock are coated by traces of iron oxide; and finally limestone type 6 is medium to coarse grain, composed mainly of calcite as major mineral constituent and represented the cement of the rock associated with some traces of opaque and talc minerals less than 10%. Talc occurs as coarse euhedral grains of subangular to subrounded outlines in the matrix of calcite. Few pores and fossils were detected in this rock. The petrographical analysis was carried out at the Key Laboratory of Mineral Resources Processing and Environment of Hubei Province, Luoshi Road 122, Wuhan, Hubei 430070, China.

2.3. Physical Characteristics. The physical parameters of the rock samples were applied according to the test methods outlined by ASTM [21] and ISRM [22], and they are determined using the saturation technique. Absorption of water is a significant parameter in determining the durability of natural rocks used as building and construction materials [23]. The presence of water strongly influences rock characteristics [24]. For this reason, the saturated mass (m_{sat}), the oven-dried mass (m_{dry}), and bulk volume (V) of rock samples were determined and then the bulk density (ρ_b), effective porosity (n_e), and water absorption (W_{abs}) of rock samples were obtained using equations (1)–(3), respectively:

$$\rho_b = \frac{m}{V}, \tag{1}$$

$$n_e = \frac{\left(m_{sat} - m_{dry}\right)}{\left(V \times \rho_w\right)} \times 100, \tag{2}$$

$$W_{abs} = \frac{\left(m_{sat} - m_{dry}\right)}{m_{dry}} \times 100, \tag{3}$$

where ρ_w is the water density. For each type of rock samples, at least five samples were prepared and tested for determining the mentioned physical properties, and then their average values were determined. The mean initial physical properties of the studied rock samples (fresh) are summarized in Table 1.

2.4. Frost Damage Test. Frost-weathering process seeks to reproduce the pressures, which may originate within the stone when water turns into ice. These influences are determined by changing the temperature below and above the freezing point of water in the specimens containing a known quantity of water [25]. To determine the durability and simulate the impact of frost action on the physical and mechanical parameters of the tested rock specimens under study, frost-weathering process was performed according to the procedures proposed by DL/T 5368 National Development and Reform Commission of the People's Republic of China [26]. According to Ruedrich et al. [7], a clear deterioration of stones used as building and construction materials cannot be identified in most cases not less than 50 cycles of weathering process have been done. In this study, 50 cycles of frost damage process were carried out on saturated rock samples including 4 hr freezing duration in air after temperature of the test chamber reaching −20°C, followed by 4 hr thawing duration in distilled water at +20°C. Each frost-weathering cycle requires 8 hr period to get completed. Rock samples after frost-weathering cycles were kept underwater until loaded in mechanical tests, but in physical properties, they were preserved for a short time. In other words, the rock specimens against frost-weathering cycles remained almost saturated. Two series of the studied samples were prepared for each rock type to determine their unconfined compressive strength, point load index strength, and Schmidt hammer rebound before and after frost-weathering cycles. The first series of rock samples were used for determining their initial properties (fresh samples), and the second series were subjected to frost-weathering cycles. After frost cycles, no visible cracks or fissures occurred in the samples; however, there is slight loss of weight less than 0.2%. After every 10 cycles of frost weathering, for mechanical properties including unconfined compressive strength, point load strength, and Schmidt hammer rebound, the measurements were made on five specimens under saturation conditions.

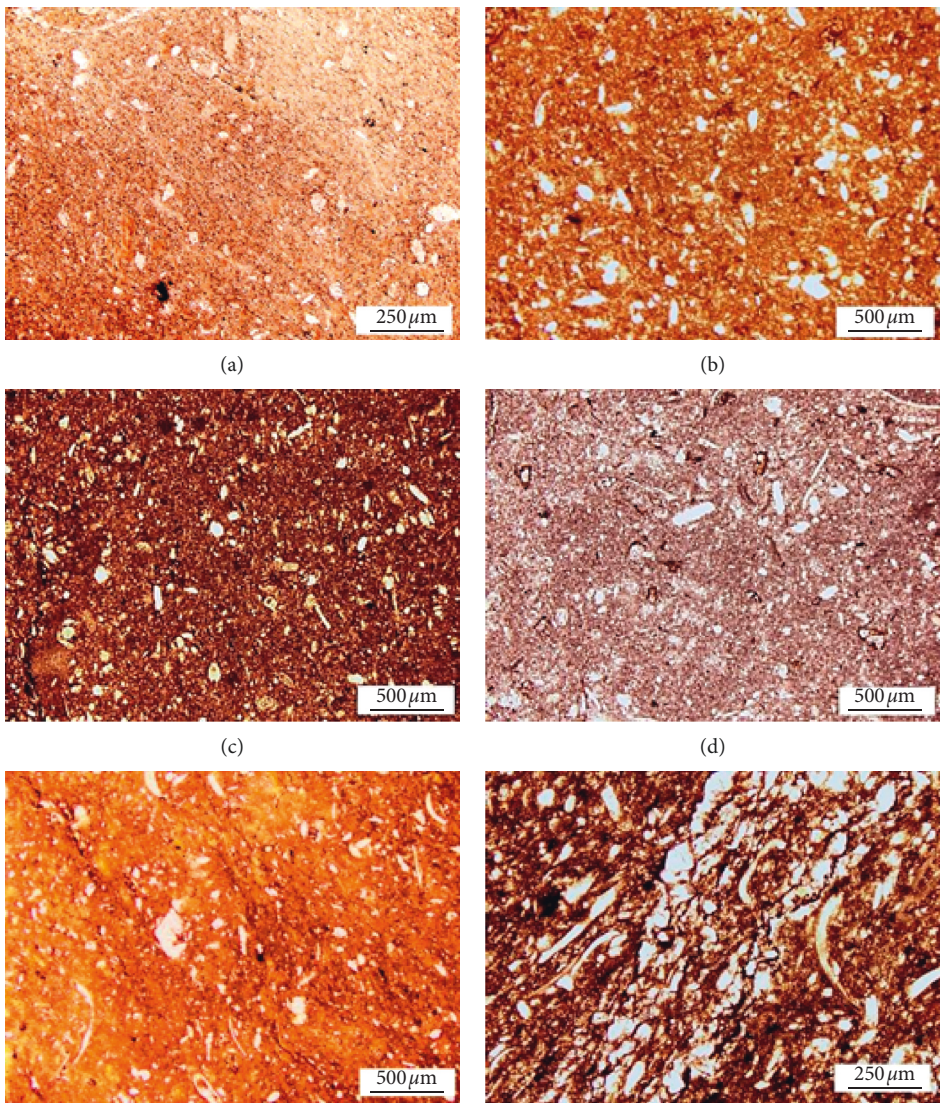

Figure 3: The microstructure of samples: (a) limestone 1; (b) limestone 2; (c) limestone 3; (d) limestone 4; (e) limestone 5; (f) limestone 6.

Table 1: Mean physical characteristics of studied rock samples.

Rock type	Dry bulk density ρ_{dry} (g/cm^3)	Saturated bulk density ρ_{sat} (g/cm^3)	Effective porosity n_e (%)	Absorption W_{aps} (%)
Limestone type 1	2.62	2.63	0.11	0.03
Limestone type 2	2.60	2.62	0.33	0.13
Limestone type 3	2.58	2.59	0.80	0.33
Limestone type 4	2.61	2.61	0.62	0.24
Limestone type 5	2.61	2.62	0.47	0.20
Limestone type 6	2.56	2.58	1.32	0.51

2.5. Mechanical Properties

2.5.1. Unconfined Compression Test. The compression test is the most important mechanical method to determine the rock strength [27, 28]. The uniaxial compressive strength of rocks subjected to the frost process is a significant index to select stones used as building elements and evaluate the stability of rock engineering in cold areas [15, 29]. Also, it provides useful information for rock durability assessment during weathering processes. The unconfined compression test performed on cylindrical specimens with the ratio between length and diameter is about 2 according to methods proposed by standard ISRM [22] and NF EN 1926 [30]. In this study, a TAW-2000 microcomputer electrohydraulic servo-controlled system was applied. The maximum loading capacity is 2000 kN, and the stress rate is between 0.1 and

0.15 kN/s with a ±1% precision. This test was performed on five samples for each rock type, and the mean values of unconfined compressive strength were obtained.

2.5.2. Point Load Test. Point load test, as one of the significant mechanical strength methods, was applied in this study. The point load method has been used as an indirect test for determining the strength of rock and has been used in practice because of their testing simplicity, the easiness of specimen preparation, and field applications [31, 32] The point load strength test was performed in accordance with the test methods procedures outlined by ISRM [31]. Axial tests were conducted on cylindrical samples with a diameter of 50 mm with the ratio between length and diameter about 0.7. For each rock type, five samples were tested, and their mean values were determined.

2.5.3. Schmidt Hammer Test. Schmidt hammer rebound of rocks was used and determined by the test methods procedures according to the technical regulation of JGJ/T23 [33]. In this study, A HT60 digital rebound hammer having impact energy of 2.207 Nm was applied. The testing side surfaces of large block specimens were smooth and clean. The Schmidt hammer device was held vertically downward position. In total, sixteen individual impacts were performed on any rock specimen, and the impact rebound values were recorded; each test location was separated by at least a plunger diameter. Finally, the average values were recorded.

The mean and standard deviation (SD) for unconfined compressive strength (UCS), point load index strength (Is (50)), and Schmidt hammer rebound hardness (Sch) values of studied rock samples before and after frost-weathering cycles are given in Tables 2–4, respectively.

2.6. Mathematical Modelling

2.6.1. Decay Function Model. After frost damage process, the deterioration rate of the studied rock specimens was assessed by the mathematical decay function approach. Although artificial weathering processes in long-term durability evaluation is widely used, numerical modeling methods are not enough to assess the results determined from the studies [20, 34, 35].

Therefore, Mutlutürk et al. [20] postulated a mathematical decay function approach using a decay constant (λ) and half-life ($N_{1/2}$) parameters to express the deterioration rate (integrity loss) of different rock samples after frost and heating-cooling weathering tests. The mathematical model proposes that the disintegration or integrity loss rate against the impacts of different artificial weathering agents is proportional to integrity of rock at the beginning of each cycle through the artificial weathering processes:

$$-\left(\frac{\mathrm{d}I}{\mathrm{d}N}\right) = \lambda I, \tag{4}$$

where ($\mathrm{d}I/\mathrm{d}N$) is the rate of disintegration, λ is the decay constant, I is the integrity of rock, and N is the cycle number. The minus sign in formula (4) shows the integrity decrease of a rock. By integrating this formula, between the major rock integrity (I_0) and the integrity after N cycles (I_N), a formula in logarithmic form is determined as

$$\int_{I_0}^{I_N}\left(\frac{\mathrm{d}I}{\mathrm{d}N}\right) = \lambda I \longrightarrow \ln\left(\frac{I_0}{I_N}\right) = \lambda N. \tag{5}$$

This relation can be expressed in the exponential form as follows:

$$I_N = I_0 e^{-\lambda N}. \tag{6}$$

The term $e^{-\lambda N}$ is the decay factor, which shows the proportion of the remaining integrity after N cycles, i.e., (I_N/I_0). Also, the decay constant (λ) shows the average relative loss of integrity by the work of any single cycle, and it can be used as a measure of long-term rock durability; the half-life ($N_{1/2}$) of the rock refers to the number of cycles necessary to decrease the integrity of rock to its half value. This parameter of durability is inversely related to the decay factor and is defined by replacing ($I_0/2$) with I_N in equation (5), and the half-life is obtained as shown below:

$$N_{1/2} = \frac{\ln 2}{\lambda} \approx \frac{0.6930}{\lambda}. \tag{7}$$

A simple regression analysis is used to obtain the decay constant (λ). Figure 4 shows that the loss of integrity of a parameter is determined in an exponential form [35].

As shown in Figure 4, the decay constant is inversely related to the integrity pattern. A sudden reduction in the integrity of a parameter (in this research, unconfined compressive strength, point load index strength, and Schmidt rebound) shows relatively high values of the decay constant and a rapid degradation rate (integrity decrease).

The values of the decay constant (λ) obtained from unconfined compressive strength, point load index strength, and Schmidt rebound of the different rock samples due to frost-weathering conditions are presented in Figures 5(a)–5(f), and the half-life ($N_{1/2}$) values calculated from equation (7) for unconfined compressive strength, point load strength, and Schmidt hammer rebound of each rock sample are presented in Tables 5–7, respectively. Johnson and Wichern [36] indicated that the degree of fit to a curve can be obtained by the coefficient of correlation value (R), which measures the proportion of difference in the dependent variable. The high values of coefficient of correlation, presented in Tables 5–7, indicate that the proposed model fits the data well and are qualified to estimate the mechanical parameters of the studied rock specimens after any frost damage cycle.

3. Discussion

The deterioration rate or integrity loss of each rock type due to frost damage action was assessed using a mathematical decay function approach parameters including the decay constant (λ) and half-life ($N_{1/2}$).

Table 2: Mean and standard deviation (SD) of unconfined compressive strength (UCS), MPa, values before and after frost cycles.

Cycles	Fresh		10		20		30		40		50	
	Mean	SD	Mean	SD	Mean	SD	Mean	SD	Mean	SD	Mean	SD
Limestone 1	92.0	11.4	90.8	10.2	88.6	12.0	88.0	11.9	85.8	13.7	84.0	15.8
Limestone 2	84.0	16.5	81.9	15.2	80.8	15.5	80.5	14.4	75.7	18.2	73.6	16.1
Limestone 3	52.7	11.8	48.1	12.6	45.1	11.5	43.6	14.0	40.1	17.2	35.8	16.0
Limestone 4	69.5	15.6	67.0	13.2	66.6	12.4	65.3	11.6	61.8	14.9	56.9	17.5
Limestone 5	74.0	7.3	67.5	11.6	65.0	12.1	62.8	15.3	60.0	14.1	56.7	12.9
Limestone 6	47.6	12.8	45.0	14.2	42.5	16.3	39.0	14.7	37.0	17.1	33.0	19.9

Table 3: Mean and standard deviation (SD) of point load index strength (Is (50)), MPa, values before and after frost cycles.

Cycles	Fresh		10		20		30		40		50	
	Mean	SD	Mean	SD	Mean	SD	Mean	SD	Mean	SD	Mean	SD
Limestone 1	6.8	0.60	6.8	0.71	6.7	0.55	6.6	0.78	6.4	0.85	6.2	0.96
Limestone 2	6.3	0.56	6.1	0.49	5.8	0.53	5.7	0.61	5.5	0.48	5.3	0.42
Limestone 3	4.8	0.44	4.6	0.56	4.5	0.39	4.3	0.47	4.0	0.59	3.6	0.51
Limestone 4	6.0	0.59	5.8	0.66	5.8	0.49	5.5	0.57	5.3	0.69	5.1	0.77
Limestone 5	5.8	0.39	5.7	0.47	5.5	0.37	5.4	0.49	5.2	0.43	4.9	0.45
Limestone 6	4.1	0.40	4.1	0.36	3.9	0.41	3.7	0.48	3.4	0.49	3.0	0.53

Table 4: Mean and standard deviation (SD) of Schmidt hammer rebound (Sch) values before and after frost cycles.

Cycles	Fresh		10		20		30		40		50	
	Mean	SD	Mean	SD	Mean	SD	Mean	SD	Mean	SD	Mean	SD
Limestone 1	55.1	2.2	54.7	2.4	54.2	2.1	53.6	2.9	52.9	1.7	52.4	2.0
Limestone 2	52.7	2.6	51.8	2.2	51.1	1.9	50.6	2.0	49.9	1.7	49.3	2.1
Limestone 3	38.4	1.3	37.8	1.4	36.9	0.9	36.2	1.1	35.0	1.6	34.3	1.8
Limestone 4	43.2	1.8	42.5	1.6	42.0	1.7	41.4	1.9	40.8	2.2	40.1	2.3
Limestone 5	49.8	2.0	49.0	2.1	48.2	2.4	47.6	1.8	46.5	2.3	45.7	1.9
Limestone 6	34.0	0.8	33.3	0.9	32.5	1.1	31.7	1.3	31.0	1.0	30.3	1.4

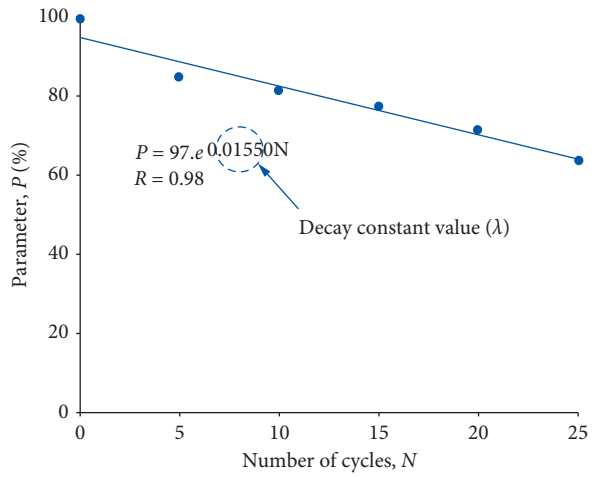

Figure 4: Determining the decay constant property (λ) from weathering processes [35].

3.1. Decay Constant (λ). The values of the decay constant for each studied rock type are given in Tables 5–7. The results indicate that the rocks of the same type do not give perfect information according to their durability under frost-weathering conditions. For instance, one of the highest durable rock specimens (limestone type 1) and also one of the least durable rock specimens (limestone type 6) under frost-weathering test (i.e., having the lowest and highest decay constant, $\lambda = -0.002$ and -0.007, respectively) (Table 5) are of the same type of rock. Indeed, limestone type 1

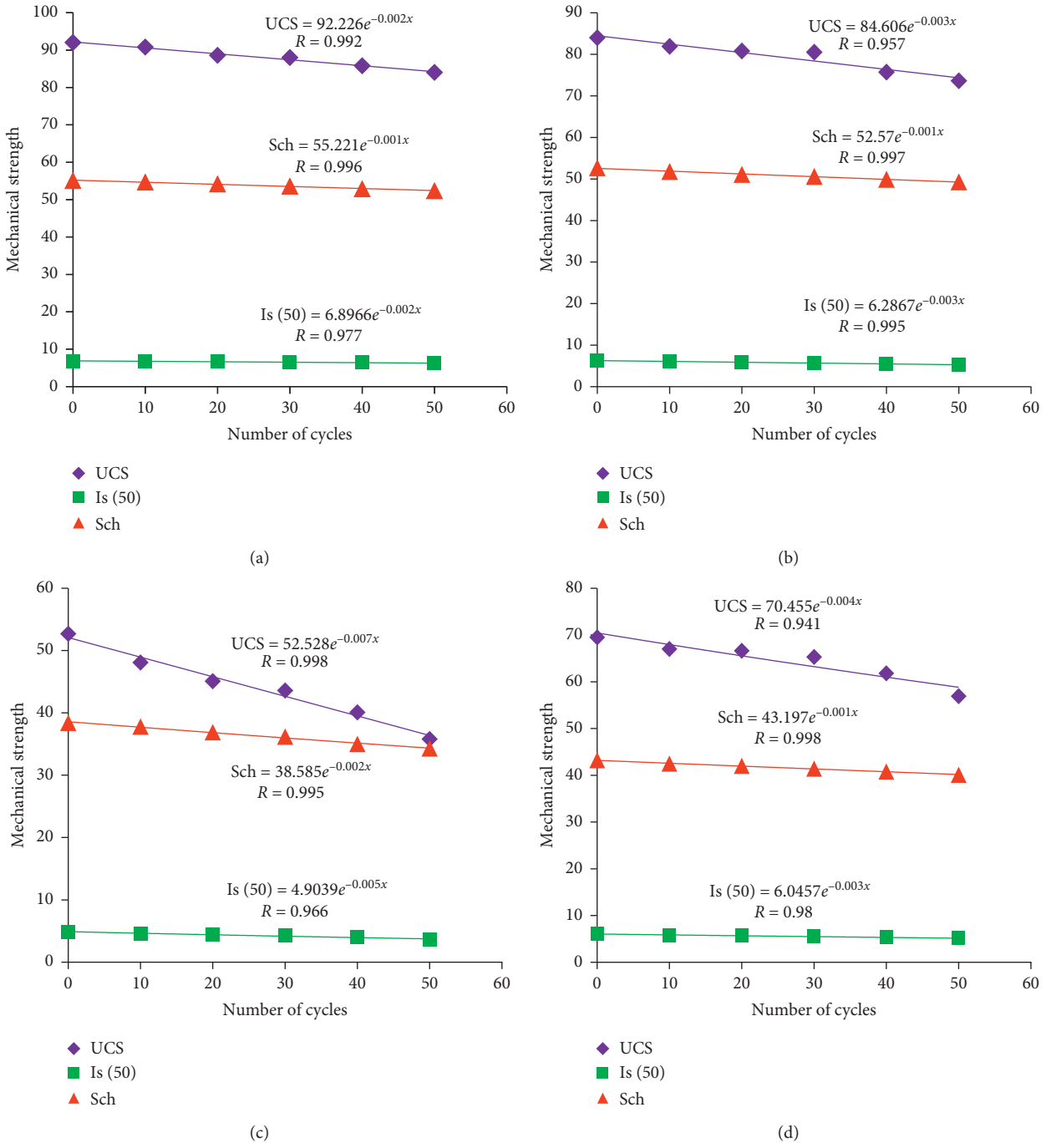

Figure 5: Continued.

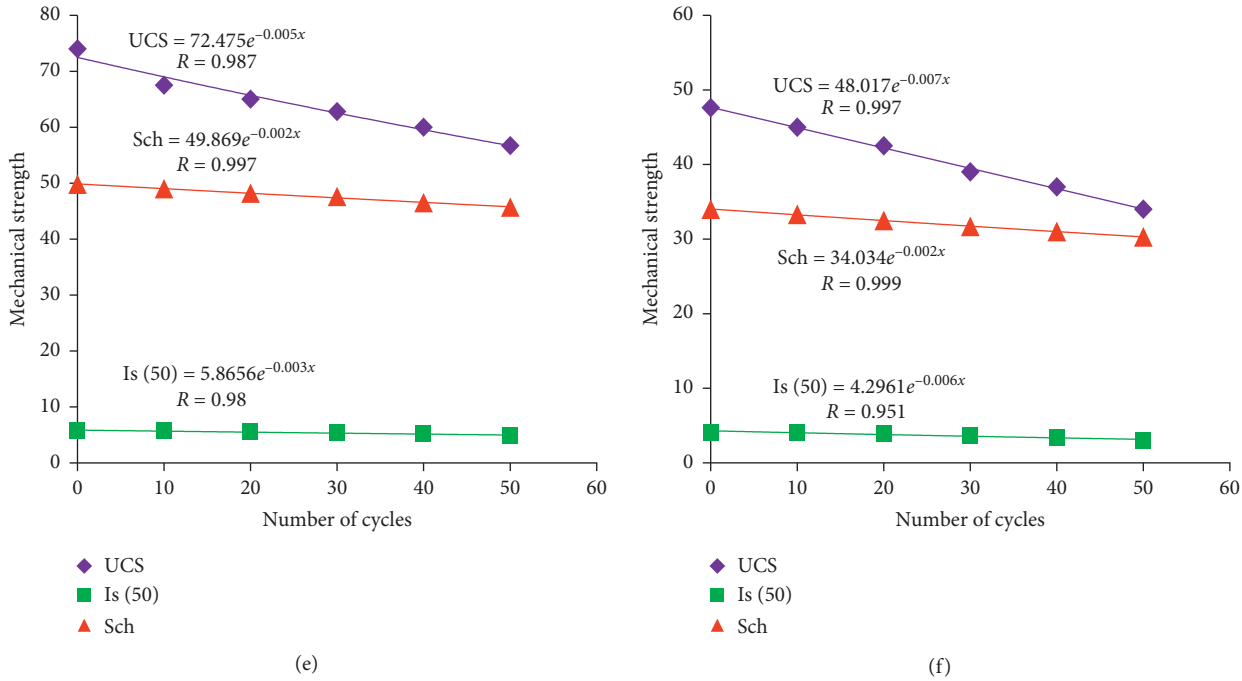

Figure 5: Determining the decay constant (λ) of samples under frost cycles: (a) limestone 1; (b) limestone 2; (c) limestone 3; (d) limestone 4; (e) limestone 5; (f) limestone 6.

Table 5: The decay constant (λ), half-life ($N_{1/2}$), and coefficient of correlation (R) of unconfined compressive strength (UCS).

Rock type	Unconfined compressive strength UCS (MPa)		
	λ	$N_{1/2}$	R
Limestone 1	−0.002	346.5	0.992
Limestone 2	−0.003	231.0	0.957
Limestone 3	−0.007	99.0	0.988
Limestone 4	−0.004	173.3	0.941
Limestone 5	−0.005	138.6	0.987
Limestone 6	−0.007	99.0	0.997

Table 6: The decay constant (λ), half-life ($N_{1/2}$), and coefficient of correlation (R) of point load index strength (I_s (50)).

Rock type	Point load index strength, I_s (50) (MPa)		
	λ	$N_{1/2}$	R
Limestone 1	−0.002	346.5	0.977
Limestone 2	−0.003	231.0	0.995
Limestone 3	−0.005	138.6	0.966
Limestone 4	−0.003	231.0	0.98
Limestone 5	−0.003	231.0	0.98
Limestone 6	−0.006	115.5	0.951

losses only 0.2% of its unconfined compressive strength value, on average, after one frost-weathering cycle, whereas limestone type 6 losses 0.7%. Consequently, the integrity loss rate (disintegration rate) of limestone type 6 is 3.5 times more than that of limestone type 1. On the contrary, some of the rock samples have same durability due to frost-weathering action. For example, limestone type 2, limestone type 4, and limestone type 5 have the same rate of integrity loss, 0.3% (i.e., $\lambda = -0.003$) (Table 6), however, indicating different physicomechanical characteristics.

Table 7: The decay constant (λ), half-life ($N_{1/2}$), and coefficient of correlation (R) of Schmidt hammer rebound (Sch).

Rock type	Schmidt hammer rebound (Sch)		
	λ	$N_{1/2}$	R
Limestone 1	−0.001	693.0	0.996
Limestone 2	−0.001	693.0	0.997
Limestone 3	−0.002	346.5	0.995
Limestone 4	−0.001	693.0	0.998
Limestone 5	−0.002	346.5	0.997
Limestone 6	−0.002	346.5	0.999

3.2. Half-Life ($N_{1/2}$). When considering the rock deterioration against recurrent frost-weathering cycles, its decay constant may refer to the rate of disintegration. But, within the state of durability of rock, the half-life, which is inversely proportional to the decay constant, is more important. Furthermore, it estimates how many cycles are required to decrease mechanical parameters to their half value; rocks that are capable to resist the frost-weathering process have higher values of half-life [37].

The values of the half-life ($N_{1/2}$) for the studied rock samples are presented in Tables 5–7 and graphically indicated in Figures 6(a)–6(c). As can be seen from Table 5 and Figure 6(a), based on unconfined compressive strength, limestone type 1 has the longest half-life (346.5 cycles), while the shortest for limestone type 3 and limestone type 6 (99

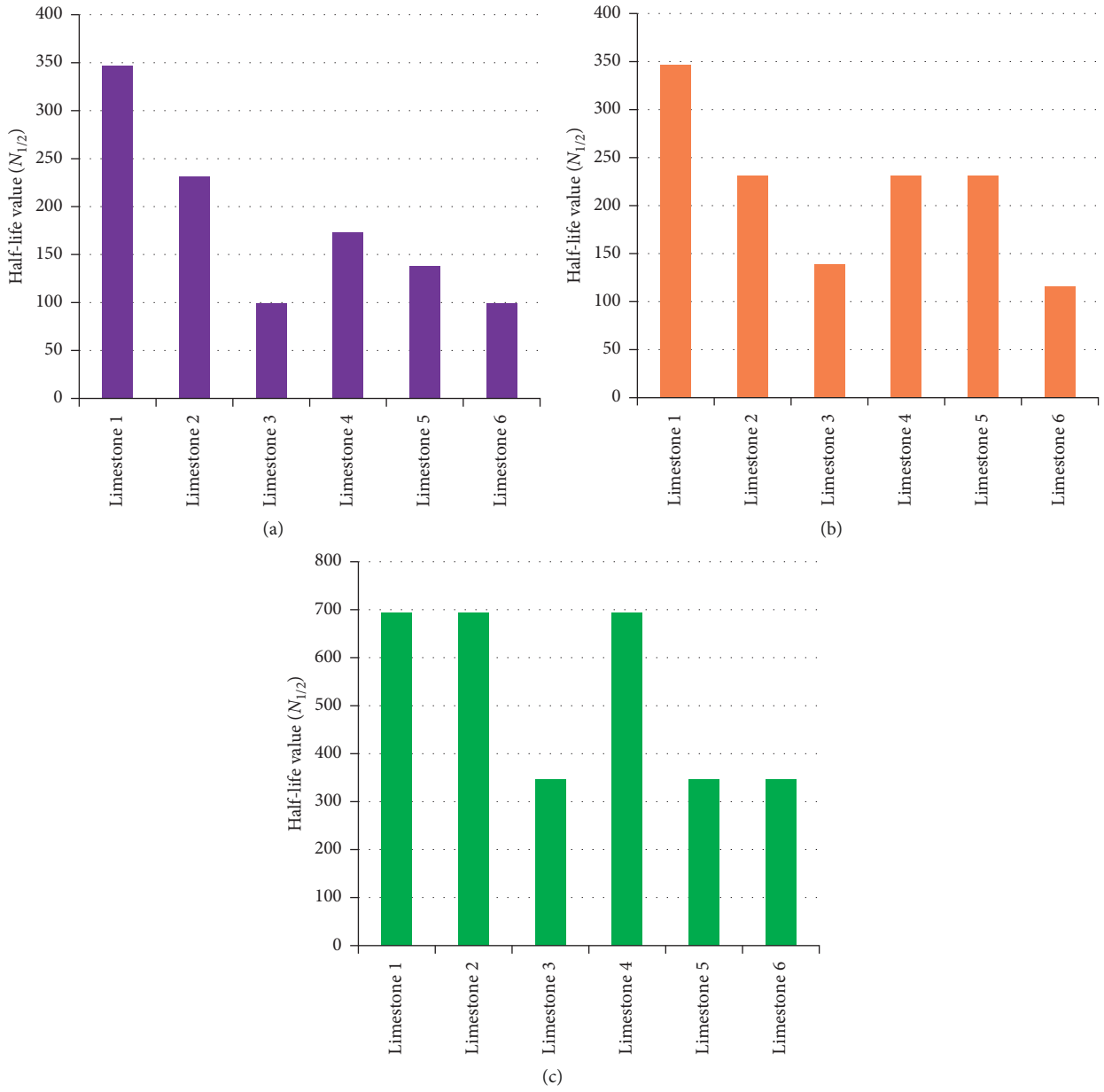

FIGURE 6: The half-life values ($N_{1/2}$) of samples: (a) unconfined compressive strength; (b) point load strength; (c) Schmidt hammer rebound.

cycles). Furthermore, Table 6 and Figure 6(b) indicate that the rock samples of limestone type 1 have the longest half-life (346.5 cycles) based on point load strength, while the rock samples, namely, limestone type 6, have the shortest half-life (115.5 cycles). Finally, as shown in Table 7 and Figure 6(c), depending on Schmidt hammer rebound, the rock samples of limestone type 1, limestone type 2, and limestone type 4 have the longest half-life (693 cycles), while it is the shortest for limestone type 3, limestone type 5, and limestone type 6 (346.5 cycles). It is significant to observe that the half-life values of all the studied rocks based on Schmidt hammer rebound are higher than those with respect to unconfined compressive strength and point load index strength. Moreover, there is no noticeable relation between mechanical strength parameters and half-life values, where we found that some of the studied rocks have the same half-life values, however indicating different petrographic, physical, and mechanical characteristics.

As mentioned previously, the durability parameter of half-life is inversely proportional to the decay factor, and their explanation should give similar conclusion. Therefore, the values of the half-life determined from the mathematical decay function approach can be used to estimate the deterioration rate of studied rock specimens under artificial frost damage conditions, using unconfined compressive strength, point load index strength, and Schmidt rebound.

In this study, the obtained values of the decay constant and half-life were compared to the previous studies (Table 8). It is observed that there is important difference between the results of this research and other previous studies.

Table 8: Comparing values of the parameters of a mathematical decay function model obtained in the present study with other studies.

Reference	Rock type	Rock properties	Decay constant (λ)	Half-life ($N_{1/2}$)
Mutlutürk et al. [20]	Various limestone samples	SH	−0.003 to −0.007	244.5 to 84.8
	Various travertine samples	SH	−0.004 to −0.007	168.2 to 101.1
Akin and Özsan [35]	Travertine[a]	UCS[c]	−0.002	288.8
	Travertine[b]	UCS[c]	−0.005	147.5
Jamshidi et al. [34]	Various limestone samples	BTS	−0.002 to −0.004	346.5 to 173.3
		Is (50)	−0.004	173.3
	Various limestone samples	BTS	−0.015 to −0.024	46.2 to 28.9
		Is (50)	− 0.019 to −0.02	36.5 to 34.7
The present study	Six different limestone types	USC	− 0.002 to −0.007	346.5 to 99
		Is (50)	−0.002 to −0.006	346.5 to 115.5
		Sch	−0.001 to −0.002	693 to 346.5

SH, shore hardness; UCS, unconfined compressive strength; BTS, Brazilian tensile strength; I_s (50), point load strength; [a]porosity <5%; [b]porosity > 5%; [c]perpendicular to lamination; Sch, Schmidt rebound hardness.

For example, the decay constant and half-life values of studied different types of limestone samples with regard to point load index values are −0.002 to −0.006 and 346.5 to 115.5, respectively, while those determined by Jamshidi et al. [34] are −0.004 and 173.3. Furthermore, the values of the parameters of λ and $N_{1/2}$ of different limestone types with respect to Schmidt rebound hardness are −0.001 to −0.002 and 693 to 346.5, respectively, while those obtained by Mutlutürk et al. [20] are −0.003 to −0.007 and 244.5 to 84.8. It is believed that the difference in the values of the decay constant and half-life determined in this work and other previous studies is maybe due to the difference in the petrographical and physico-mechanical characteristics of the rock specimens used; the parameter of integrity; the number of frost-weathering cycles; and the period time of each frost cycle.

Figures 6(a)–6(c) present that those half-life values have no meaningful pattern with regard to the rock type. Indeed, rocks with respect to the same origin can display a clear various durability under frost-weathering conditions in some cases. Therefore, the type of rock itself cannot give sufficient information regarding the durability of rock specimens due to frost-weathering action. For example, limestone sample types 4 and 5 (Figure 6) have different values of half-life based on unconfined compressive strength and Schmidt hammer rebound, and this is due to difference in microstructure features (Figure 3) and physico-mechanical properties. On the contrary, the same types of these samples have the same half-life values according to the point load index strength. Hence, the type of rock alone does not give clue for the half-life of stones used as construction materials under frost action. The results are consistence with the findings of Eren and Bahali [38] and Mutlutürk et al. [20]. Eren and Bahali [38] determined the decrease in weight of two different types of limestone specimens after frost-weathering test. They observed that the rocks with regard to the same origin could display clearly different behaviours under frost-weathering action and this is due to difference in their porosity. Mutlutürk et al. [20] measured the shore hardness variations of some different rock types against frost-weathering cycles. They indicated that the type of rock alone does not provide clue for the half-life of rocks used as building stones and construction materials under frost cycles.

4. Conclusions

In this work, the frost damage test up to 50 cycles was performed on six different limestone types used as building and construction materials to assess their long-term durability by the mathematical decay function approach. The model gives two important properties such as decay constant (λ) and half-life ($N_{1/2}$) to estimate the integrity loss or deterioration rate of rocks under frost damage conditions. Therefore, these significant parameters save a lot of time and provide important practical features to assess fast long-term durability. The mathematical model showed response of all the studied different rock samples to frost-weathering process. The parameters of the decay function model obtained are in good accuracy to estimate the disintegration rate of studied rocks, and hence, there is no need to carry out the artificial frost-weathering test which is slow and consumes a lot of time, and this is suitable for rocks of the same type especially which were extracted from the same areas because of its near physical and mechanical characteristics. Some of studied rocks have the same half-life values but indicating different petrographical, physical, and mechanical characteristics, and hence, there is no clear relation between mechanical strength parameters and half-life values. In this work, we can also conclude that half-life has no purposeful pattern according to the type of rock. On the contrary, the rock type itself cannot give any index or clue for the long-term durability of rock samples used here under frost damage process. This model also confirmed that the disintegration rate was higher with unconfined compressive strength and point load index strength compared with that resulting from Schmidt rebound of studied rocks under frost damage conditions.

This work has important progress on the durability properties of carbonate building materials such as limestone and innovates a paradigm for the next researches for the prediction of integrity loss or disintegration rate of the rocks due to frost damage process by using numerical modeling technique (mathematical decay function approach) which saves a lot of time, and hence, there is no need to carry out the frost test which is slow and consumes the time. However, to obtain more significant results in the prediction of the deterioration rate of natural rocks used as building stones

and construction materials under frost damage process, the future studies should use different rock origins under different environmental conditions and establish another model with different tests.

Data Availability

The data used to support the findings of this study are included within the article.

Conflicts of Interest

The authors declare that there are no conflicts of interest regarding the publication of this paper.

Acknowledgments

This work was supported by the National Key R&D Plan under Grant nos. 2018YFC0808405 and 2018YFC0604401 and the Natural Science Foundation of China under Grant no. 51774220.

References

[1] Z. Zhou, X. Cai, D. Ma, L. Chen, S. Wang, and L. Tan, "Dynamic tensile properties of sandstone subjected to wetting and drying cycles," *Construction and Building Materials*, vol. 182, pp. 215–232, 2018.

[2] M. Á. García-del-Cura, D. Benavente, J. Martínez-Martínez, and N. Cueto, "Sedimentary structures and physical properties of travertine and carbonate tufa building stone," *Construction and Building Materials*, vol. 28, no. 1, pp. 456–467, 2012.

[3] D. Eren Sarici, "Thermal deterioration of marbles: gloss, color changes," *Construction and Building Materials*, vol. 102, pp. 416–421, 2016.

[4] Z. Zhou, X. Cai, L. Chen, W. Cao, Y. Zhao, and C. Xiong, "Influence of cyclic wetting and drying on physical and dynamic compressive properties of sandstone," *Engineering Geology*, vol. 220, pp. 1–12, 2017.

[5] J. Yu, X. Chen, H. Li, J.-W. Zhou, and Y.-Y. Cai, "Effect of freeze–thaw cycles on mechanical properties and permeability of red sandstone under triaxial compression," *Journal of Mountain Science*, vol. 12, no. 1, pp. 218–231, 2015.

[6] C. M. Grossi, P. Brimblecombe, and I. Harris, "Predicting long term freeze–thaw risks on Europe built heritage and archaeological sites in a changing climate," *Science of the Total Environment*, vol. 377, no. 2-3, pp. 273–281, 2007.

[7] J. Ruedrich, D. Kirchner, and S. Siegesmund, "Physical weathering of building stones induced by freeze–thaw action: a laboratory long term study," *Environmental Earth Sciences*, vol. 63, no. 7-8, pp. 1573–1586, 2011.

[8] A. B. Yavuz, C. Akal, N. Türk, M. Çolak, and B. F. Tanyu, "Investigation of discrepancy between tuff used as building stones in historical and modern buildings in western Turkey," *Construction and Building Materials*, vol. 93, pp. 439–448, 2015.

[9] J. Park, C.-U. Hyun, and H.-D. Park, "Changes in microstructure and physical properties of rocks caused by artificial freeze–thaw action," *Bulletin of Engineering Geology and the Environment*, vol. 74, no. 2, pp. 555–565, 2015.

[10] M. Takarli, W. Prince, and R. Siddique, "Damage in granite under heating/cooling cycles and water freeze–thaw condition," *International Journal of Rock Mechanics and Mining Sciences*, vol. 45, no. 7, pp. 1164–1175, 2008.

[11] G. Khanlari and Y. Abdilor, "Influence of wet–dry, freeze–thaw, and heat–cool cycles on the physical and mechanical properties of upper red sandstones in central Iran," *Bulletin of Engineering Geology and the Environment*, vol. 74, no. 7, pp. 1287–1300, 2014.

[12] A. Jamshidi, M. R. Nikudel, and M. Khamehchiyan, "A novel physicomechanical parameter for estimating the mechanical strength of travertines after a freeze–thaw test," *Bulletin of Engineering Geology and the Environment*, vol. 76, no. 1, pp. 181–190, 2017.

[13] C. Di Benedetto, P. Cappelletti, M. Favaro et al., "Porosity as key factor in the durability of two historical building stones: neapolitan yellow tuff and Vicenza stone," *Engineering Geology*, vol. 193, pp. 310–319, 2015.

[14] P. Vázquez, F. J. Alonso, L. Carrizo et al., "Evaluation of the petrophysical properties of sedimentary building stones in order to establish quality criteria," *Construction and Building Materials*, vol. 41, pp. 868–878, 2013.

[15] F. Bayram, "Predicting mechanical strength loss of natural stones after freeze–thaw in cold regions," *Cold Regions Science and Technology*, vol. 83-84, pp. 98–102, 2012.

[16] Z. Karaca, A. Hamdi Deliormanli, H. Elci, and C. Pamukcu, "Effect of freeze–thaw process on the abrasion loss value of stones," *International Journal of Rock Mechanics and Mining Sciences*, vol. 47, no. 7, pp. 1207–1211, 2010.

[17] X. Tan, W. Chen, and J. Cao, "Laboratory investigations on the mechanical properties degradation of granite under freeze–thaw cycles," *Cold Regions Science and Technology*, vol. 68, no. 3, pp. 130–138, 2011.

[18] H. Yavuz, R. Altindag, S. Sarac, I. Ugur, and N. Sengun, "Estimating the index properties of deteriorated carbonate rocks due to freeze–thaw and thermal shock weathering," *International Journal of Rock Mechanics and Mining Sciences*, vol. 43, no. 5, pp. 767–775, 2006.

[19] L. M. O. Sousa, L. M. Suárez del Río, L. Calleja, V. G. Ruiz de Argandoña, and A. R. Rey, "Influence of micro fractures and porosity on the physico-mechanical properties and weathering of ornamental granites," *Engineering Geology*, vol. 77, no. 1-2, pp. 153–168, 2005.

[20] M. Mutlutürk, R. Altindag, and G. Türk, "A decay function model for the integrity loss of rock when subjected to recurrent cycles of freezing-thawing and heating–cooling," *International Journal of Rock Mechanics and Mining Sciences*, vol. 41, no. 2, pp. 237–244, 2004.

[21] ASTM, *Standard Test Method for Density, Relative Density (Specific Gravity), and Absorption of Coarse Aggregate*, Annual Book of ASTM Standards, West Conshohocken, PA, USA, 2001.

[22] ISRM, *Rock Characterization, Testing, and monitoring. ISRM Suggested Methods*, Pergamon Press, Oxford, UK, 1981.

[23] A. Shakoor and R. E. Bonelli, "Relationship between petrophysical characteristics, engineering index properties and mechanical properties of selected sandstones," *Environmental & Engineering Geoscience*, vol. xxviii, no. 1, pp. 55–71, 1991.

[24] X. Cai, Z. Zhou, K. Liu, X. Du, and H. Zang, "Water-weakening effects on the mechanical behavior of different rock types: phenomena and mechanisms," *Applied Sciences*, vol. 9, no. 20, p. 4450, 2019.

[25] P. R. Rossi-Doria, *Laboratory Tests on Artistic Stonework. Studies and Documents on the Cultural Heritage*, UNESCO, Paris, France, 1985.

[26] National Development and Reform Commission of the People's Republic of China, *Code for Rock Tests of Hydroelectric and Water Conservancy Engineering, (DL/T 5368-2007)*, Vol. 11-12, National Development and Reform Commission of the People's Republic of China, Beijing, China, 2007.

[27] Z. Zhou, X. Cai, X. Li, W. Cao, and X. Du, "Dynamic response and energy evolution of sandstone under coupled static–dynamic compression: insights from experimental study into deep rock engineering applications," *Rock Mechanics and Rock Engineering*, vol. 1-27, 2019.

[28] M. Kou, X. Liu, S. Tang, and Y. Wang, "3-D X-ray computed tomography on failure characteristics of rock-like materials under coupled hydro-mechanical loading," *Theoretical and Applied Fracture Mechanics*, vol. 104, Article ID 102396, 2019.

[29] Q. Liu, S. Huang, Y. Kang, and X. Liu, "A prediction model for uniaxial compressive strength of deteriorated rocks due to freeze–thaw," *Cold Regions Science and Technology*, vol. 120, pp. 96–107, 2015.

[30] UNE-EN 1926, *Natural Stone Tests Methods. Determination of Uniaxial Compressive Strength*, European Committee for Standardization, Bruxelles, Belgium, 2007.

[31] ASTM, *Standard Test Method for Determination of the Point Load Strength Index of Rock and Application to Rock Strength Classifications*, ASTM Publication, West Conshohocken, PA, USA, 2008.

[32] J. A. Franklin, "Suggested method for determining point load strength," *International Journal of Rock Mechanics and Mining Sciences*, vol. 22, no. 2, pp. 53–60, 1985.

[33] JGJ/T23-2011, *Technical Specification for Inspection of Concrete Compressive Strength by Rebound Method, Industrial Standard of the People's Republic of China*, China, 2011.

[34] A. Jamshidi, M. R. Nikudel, and M. Khamehchiyan, "Predicting the long-term durability of building stones against freeze–thaw using a decay function model," *Cold Regions Science and Technology*, vol. 92, pp. 29–36, 2013.

[35] M. Akin and A. Özsan, "Evaluation of the long-term durability of yellow travertine using accelerated weathering tests," *Bulletin of Engineering Geology and the Environment*, vol. 70, no. 1, pp. 101–114, 2011.

[36] R. A. Johnson and D. W. Wichern, *Applied Multivariate Statistical Analysis*, Prentice-Hall, Englewood Cliffs, NJ, USA, 5th edition, 1999.

[37] M. H. Ghobadi, A. R. Taleb Beydokhti, M. R. Nikudel, A. Asiabanha, and M. Karakus, "The effect of freeze–thaw process on the physical and mechanical properties of tuff," *Environmental Earth Sciences*, vol. 75, p. 846, 2016.

[38] Ö. Eren and M. Bahali, "Some engineering properties of natural building cut stones of Cyprus," *Construction and Building Materials*, vol. 19, no. 3, pp. 213–222, 2005.